HHS Public Access

Author manuscript

Cell Rep. Author manuscript; available in PMC 2015 October 16.

Published in final edited form as:

Cell Rep. 2015 October 13; 13(2): 440–449. doi:10.1016/j.celrep.2015.09.007.

Akt kinase-mediated checkpoint of cGAS DNA sensing pathway

Gil Ju Seo[1], **Aerin Yang**[3], **Brandon Tan**[1], **Sungyoon Kim**[3], **Qiming Liang**[1], **Younho Choi**[1], **Weiming Yuan**[1], **Pinghui Feng**[1], **Hee-Sung Park**[3], and **Jae U. Jung**[1,2,*]

[1]Department of Molecular Microbiology and Immunology, Keck School of Medicine, University of Southern California, Los Angeles, California 90033, USA

[2]Department of Pharmacology and Pharmaceutical Sciences, School of Pharmacy, University of Southern California, Los Angeles, California 90033, USA

[3]Department of Chemistry, Korea Advanced Institute of Science and Technology, Daejeon, Republic of Korea

SUMMARY

Upon DNA stimulation, cyclic GMP-AMP synthetase (cGAS) synthesizes the second messenger cyclic GMP-AMP (cGAMP) that binds to the STING, triggering antiviral interferon-β (IFN-β) production. However, it has remained undetermined how hosts regulate cGAS enzymatic activity after the resolution of DNA immunogen. Here, we show that Akt kinase plays a negative role in cGAS-mediated anti-viral immune response. Akt phosphorylated the S291 or S305 residue of the enzymatic domain of mouse or human cGAS, respectively, and this phosphorylation robustly suppressed its enzymatic activity. Consequently, expression of activated Akt led to the reduction of cGAMP and IFN-β production and the increase of herpes simplex virus 1 replication, whereas treatment with Akt inhibitor augmented cGAS-mediated IFN-β production. Furthermore, expression of the phosphorylation-resistant cGAS S291A mutant enhanced IFN-β production upon DNA stimulation, HSV-1 infection, and vaccinia virus infection. Our study identifies an Akt kinase-mediated checkpoint to fine-tune hosts' immune responses to DNA stimulation.

INTRODUCTION

Innate immune receptors detect pathogens through pathogen-associated molecular patterns (PAMPs) and then elicit an immune response (Elinav et al., 2011; Medzhitov and Janeway, 2000). These germ-line-encoded pattern recognition receptors (PRR) monitor extracellular, endosomal, and intracellular compartments for molecular signatures of microbial infection or the sometimes overlapping molecular triggers produced by abnormal, damaged, or dying

*Corresponding author: Jae U. Jung, Department of Molecular Microbiology and Immunology, University of Southern California, Keck School of Medicine, Harlyne J. Norris Cancer Research Tower, 1450 Biggy Street, NRT Room 5512, Los Angeles, CA 90033, Phone (323) 442-1710, Fax (323) 442-1721, jaeujung@med.usc.edu.

AUTHOR CONTRIBUTIONS

GJS, AY, BT, SK, QL, and YC contributed to the experiments in this manuscript. WY, PF, H-SP, and JUJ designed the study. GJS and JUJ wrote the manuscript.

cells (Latz, 2010). Microbe-derived nucleic acids are potent cytosolic PAMPs that are recognized by host pattern recognition receptors such as the Toll-like receptors (TLRs) and cytosolic DNA/RNA recognition receptors (Kawai and Akira, 2011). The appearance of naked DNA in the cytoplasm of mammalian cells triggers a cellular response initiated by the DNA sensing pathway (Paludan and Bowie, 2013). Cytoplasmic DNA is recognized as foreign or indicative of cellular distress because nuclear and mitochondrial membranes typically surround self-DNAs. Many DNA sensors in the cytoplasm have been identified, including AIM2 (Fernandes-Alnemri et al., 2009; Hornung et al., 2009; Roberts et al., 2009), DAI (Takaoka et al., 2007), DDX41 (Zhang et al., 2011), DNA-PK (Ferguson et al., 2012), IFI16 (Unterholzner et al., 2010), and a form of RNA polymerase III that detects AT-rich DNA (Ablasser et al., 2009; Chiu et al., 2009). Chronic or deregulated activation of nucleic acid sensing has been shown to contribute to both microbial pathogenesis and autoimmune diseases (Liu et al., 2014; Munz et al., 2009).

Recently, cyclic GMP-AMP synthase (cGAS) was characterized as a primary cytosolic DNA sensor that triggers type I interferons (IFNs) and other inflammatory cytokines such as TNF-α and IL-6 upon DNA transfection and DNA virus infection (Li et al., 2013; Sun et al., 2013). Following activation, cGAS converts ATP and GTP into the dinucleotide cyclic GMP-AMP (cGAMP) (Gao et al., 2013b; Kranzusch et al., 2013; Wu et al., 2013). cGAMP is a second messenger that binds to STING, which in turn induces the recruitment of TANK-binding kinase 1 (TBK1) and interferon regulatory factor-3 (IRF-3) to form a complex with STING (Ablasser et al., 2013; Wu et al., 2013). The activation of IRF-3 and/or NF-kappaB signaling pathways induce the expression of type I IFNs and proinflammatory cytokines. Current structural and genetic insights into cGAS have focused on its DNA sensing mechanism and activation. However, it is not well understood how cGAS activity is negatively regulated following activation. Since both self and non-self DNA can activate cGAS, it is important to tightly regulate this DNA sensing pathway to prevent harmful activity arising from unrestrained signaling (Bhat and Fitzgerald, 2014). We have recently reported that the autophagy protein Beclin-1 negatively regulates cGAS function: the direct interaction between cGAS and Beclin-1 not only suppresses cGAMP synthesis to halt IFN production induced by dsDNA stimulation or herpes simplex virus-1 (HSV-1) infection, but also enhances the autophagy-mediated degradation of cytosolic pathogen DNAs to avoid persistent immune stimulation (Liang et al., 2014). Thus, identifying cellular pathways involved in maintaining a balanced cGAS response is the primary goal of this study.

The protein kinase Akt is one of the most critical and versatile protein kinases in higher eukaryotes. Numerous Akt substrates have been identified in relation to metabolism, cell survival, proliferation, and cell migration (Manning and Cantley, 2007). In addition, Akt may play a role in regulating the IFN pathway. Mouse fibroblasts treated with type I IFN have activated Akt that stimulates mammalian target of rapamycin (mTOR), which is an upstream regulator of IFN-stimulated gene (ISG) translation (Kaur et al., 2008a). Phosphatidylinositol 3-kinase (PI3K), an Akt upstream lipid kinase, is activated by type I and type II IFN receptors. Also, p85α and p85β, the regulatory subunits of PI3K, both cooperate to promote IFN-induced transcription and translation of ISGs (Kaur et al., 2008b). However, it still remains a question whether Akt directly controls an upstream mediator of IFN production or pattern recognition pathway. Here, we identify a molecular mechanism in

which Akt kinase negatively regulates cGAS activity. We show that Akt phosphorylates the S291 or S305 of the carboxyl-terminal enzymatic domain of mouse or human cGAS, respectively, and that this phosphorylation robustly suppresses cGAS enzymatic activity. We further reveal that this phosphorylation is a key regulatory event that inhibits cGAS enzymatic activity, leading to decreased cytokine production and antiviral activity towards DNA stimulation and DNA virus infection.

RESULTS

Akt phosphorylates cGAS

To investigate the molecular mechanism that regulates cGAS enzymatic activity, we explored the post-translational modifications of cGAS by mass spectrometry. Immunoprecipitated cGAS from 293T cells transiently expressing Flag-tagged human cGAS was resolved by SDS-PAGE and analyzed by mass spectrometry. We found that human cGAS was phosphorylated at S305 when overexpressed in 293T cells (Figure S1A). Interestingly, the sequence around S305 includes a known target motif for Akt kinase (R/KXR/KXX*S/T; X, any amino acid) (Figure 1A) that is highly conserved across multiple species. (Figure S1B). In mouse cGAS, the homologous residue is S291. Due to the proximity of S305 or S291 to the catalytic site of human or mouse cGAS, respectively, we hypothesized that Akt mediates phosphorylation at this site to control cGAS enzymatic activity. To validate Akt-mediated phosphorylation, human or mouse cGAS-Flag was transiently expressed in 293T cells, followed by treatment with Akt1/2-specific inhibitor VIII or DMSO as a control. We resolved the proteins using an SDS-PAGE gel and immunoblotted with the Akt phosphosubstrate antibody that specifically recognizes the phosphorylated consensus motif K/RXK/RXXpS/pT. Both mouse and human cGAS proteins were readily detected by the Akt phosphosubstrate antibody, which apparently disappeared upon treatment with Akt inhibitor VIII (Figures 1B and S2). However, when the phosphorylation resistant S291A mutant of mouse cGAS was expressed, it was not recognized by the anti-Akt phosphosubstrate antibody (Figure 1C). Furthermore, Akt's three isoforms (Akt1, 2, and 3) were capable of phosphorylating mouse cGAS at equivalent levels (Figure 1D). Finally, to address whether Akt directly phosphorylates cGAS as a substrate, we purified a fragment of mouse cGAS corresponding to the catalytic region (aa161–522) fused to maltose binding protein (MBP) in a bacterial expression vector. A bacterially purified GSK protein was included as a positive control. An *in vitro* kinase assay revealed that active Akt phosphorylated the cGAS WT fragment, but not the S291A mutant fragment, at the equivalent level as seen with GSK as a substrate (Figure 1E). Taken together, these results demonstrate that Akt phosphorylates the S291 residue or S305 residue of mouse or human cGAS, respectively.

Serine phosphorylation negatively regulates cGAS function

Because cGAS phosphorylation occurs close to its catalytically important residues (E211, D213 and E302), we tested whether Akt-mediated phosphorylation could affect cGAS enzyme activity. To test our hypothesis, we utilized the specific cotranslational phosphoserine (Sep) incorporation system for the S291 residue of mouse cGAS (Lee et al., 2013; Park et al., 2011). Sep, the most abundant phosphoamino acid in the eukaryotic

phosphoproteome, is not encoded in the genetic code, but is synthesized post-translationally. An *Escherichia coli* strain was genetically engineered to harbor a Sep-accepting transfer RNA ($tRNA^{Sep}$), its cognate phosphoseryl–tRNA synthetase (SepRS), and an engineered EF-Tu (EF-Sep) of *Methanocaldococcus jannaschii*. The *E. coli* strain was then transformed with bacterial expression vector containing the His-tagged mouse cGAS fragment (aa161–522), and the non-natural Sep-incorporated pS291 (directed by UAG) mutant (Figure 2A). We purified both the natural His-tagged mouse cGAS fragment and the non-natural amino acid Sep-incorporated pS291 fragment from *E. coli* (Figures 2B and 2C) and measured the fragments' NTase activity *in vitro*. While cGAMP production was efficient by mouse cGAS WT, the phosphorylated (pS291) cGAS showed a nearly complete loss of cGAMP production (Figure 2D), suggesting that S291 phosphorylation negatively regulates cGAS enzymatic activity.

To explore whether this serine phosphorylation affects cGAS-mediated signaling activity, Flag-tagged human cGAS, mouse cGAS, and their phosphorylation-resistant mutants (human cGAS S305A and mouse cGAS S291A) were stably expressed in L929 mouse fibrosarcoma cGAS−/− cells. Phosphorylation-resistant cGAS-Flag mutant-expressing cells showed substantially higher IFN-β and IL-6 expression upon DNA stimulation than cGAS-Flag WT-expressing cells (Figures 3A–3D), which was specific for DNA stimulation since only poly I:C stimulation led to equivalent levels of IFN-β and IL-6 induction in all three L929 cell lines irrespective of cGAS expression and phosphorylation (Figure 3E and unpublished results). Finally, both bacterially purified mouse cGAS WT and S291A proteins showed similar cGAMP production activity *in vitro* (Figure 3F), suggesting that the lower signaling activity of cGAS WT compared to cGAS S291A mutant appears to be due to its susceptibility to phosphorylation, but not due to its weak enzymatic activity. Collectively, these results demonstrate that the phosphorylation of S291 or S305 dampens cGAS enzymatic activity, negatively affecting its anti-viral and pro-inflammatory cytokine production.

Negative regulation of cGAS is mediated by Akt

To test the effect of Akt-mediated phosphorylation on cGAS function, the myristorylated Akt1 (myr-Akt1, constitutively active form) or the kinase dead Akt1 (KD) mutant was expressed in RAW 264.7 cells, followed by DNA stimulation or HSV-1 infection. This showed that upon DNA stimulation or HSV-1 infection, cells expressing myr-Akt1 had significantly reduced IFN-β expression compared to cells expressing Akt1 KD mutant or vector alone (Figures 4A and S3A). Additionally, myr-Akt1 expression led to the drastic reduction of cGAS-induced IFN-β promoter activity (Figure 4B). When myr-Akt1 was expressed in cGAS−/− cells complemented with vector, mouse cGAS WT, or cGAS S291A, it robustly suppressed HT-DNA stimulation-induced IFN-β expression in L929 cGAS−/− cells complemented with cGAS WT, but not in L929 cGAS−/− cells complemented with cGAS S291A mutant (Figure 4C). Furthermore, when these cells were treated with the Akt1/Akt2-specific inhibitor VIII, the Akt inhibitor apparently potentiated DNA stimulation-induced IFN-β mRNA expression (Figures 4D and S3B). To test whether Akt1 affects the cGAS downstream cascade, STING agonist, cyclic GAMP (cGAMP), was transfected into the cGAS−/− cells complemented with vector, mouse cGAS WT, or cGAS S291A in the

presence or absence of Akt inhibitor. IFN-β transcripts and proteins levels were similar after cGAMP treatment irrespective of Akt inhibitor treatment (Figures S3C and S3D). It revealed that Akt specifically inhibited cGAS signaling ability through regulating its enzyme activity. Finally, to directly address whether Akt1-mediated phosphorylation suppresses cGAS enzymatic activity, bacterially purified catalytic region (aa161–522) of mouse cGAS was mixed with catalytically active Akt1 *in vitro* and the mixtures were then subjected to cGAMP production assay. This revealed that increasing amounts of Akt1 led to decreasing production of cGAS-mediated cGAMP *in vitro*, whereas the addition of maltose binding protein (MBP) as a control showed only a slight effect on cGAMP production (Figure 4E). S291A protein resiliently produced cGAMP in the presence of Akt1, while cGAS wild type produced undetectable levels of cGAMP in the same conditions (Figure S4A). After HT-DNA and/or Akt inhibitor treatment, L929 cell lysates were added into digitonin-permeabilized THP1-Lucia™ ISG reporter cells to perform cGAMP bio-assay. This showed the significant increase of IFN responsiveness upon Akt inhibitor treatment (Figure S4B). In summary, the Akt1 kinase directly phosphorylates mouse cGAS at the S291 residue, leading to the inhibition of cGAS enzymatic activity and the suppression of cGAS-mediated IFN-β production.

Akt antagonizes cGAS-mediated IFN response upon infection with DNA viruses

To assess whether Akt antagonizes cGAS-mediated IFN response upon infection with DNA viruses, L929 cGAS −/− cells complemented with vector, mouse cGAS WT, or cGAS S291A were infected with mock or F strain HSV-1 WT or HSV-1 ΔICP34.5 mutant or the Modified Vaccina Ankara (MVA), followed by the measurement of IFN-β mRNA production. HSV-1 ΔICP34.5 mutant strain was included as a control since the GADD34 homology-containing ICP34.5 effectively counteracts the type I IFN response by binding four cellular proteins, Beclin-1, tank-binding kinase 1 (TBK1), protein phosphatase 1α (PP1α), and eukaryotic translation initiation factor 2α (eIF2α) (Kanai et al., 2012; Li et al., 2011; Orvedahl et al., 2007). As previously shown (Liang et al., 2014), expression of cGAS WT induced much higher amounts of IFN-β mRNA upon HSV-1 ΔICP34.5 infection than upon HSV-1 infection. Also, expression of the phosphorylation-resistant cGAS S291A led to substantially higher IFN-β mRNA production under the same conditions (Figures 5A and 5B). Modified Vaccina Ankara (MVA) infection also induced much higher amounts of IFN-β mRNA when cells expressing cGAS S291A compared to cells expressing cGAS WT (Figure S5A). Next, we determined whether cGAS is phosphorylated by virus infection. We analyzed cGAS phosphorylation upon HSV-1 infection in a time course. cGAS was phosphorylated at 8 hours post infection and continued to be phosphorylated 24 hours post infection (Figure S5B). Interestingly, the kinetics of cGAS phosphorylation were similar to those of Akt activation as marked by pAkt S473. Treatment of the Akt1/Akt2-specific inhibitor VIII further potentiated HSV-1-stimulated IFN-β mRNA production (Figure 5C) and we also measured the IFN-β production of L929 cells complemented with cGAS WT or S291A upon HSV-1 infection after Akt inhibitor treatment in a time course manner. IFN-β transcripts gradually increased in L929 cells complemented with phosphorylation resistant mutant S291A irrespective of Akt inhibitor treatment in the different time points, while L929 cells complemented with mouse cGAS WT peaked at 12 hours and then slightly decreased. Akt inhibitor gradually increased IFN-β transcripts in L929 cells complemented

with mouse cGAS WT (Figure S5C). The effect of either cGAS function or its Akt phosphorylation on IFN-β induction was specific to HSV-1 infection since its activity was not observed upon vesicular stomatitis virus (VSV) infection (Figure 5D).

Finally, we sought to determine how Akt1 phosphorylation affects viral replication. L929 cGAS−/− cells complemented with vector, mouse cGAS WT, or cGAS S291A were infected with HSV-1 or VSV and the viral titers produced were measured at different time points up to 48 hours post-infection using a standard plaque formation assay on Vero cells (Figures 6A and 6B). While mouse cGAS WT expression restricted HSV-1 replication compared to the vector control, cGAS S291A mutant expression led to the pronouncedly augmented restriction of HSV-1 replication (Figure 6A). Since HSV-1 Δ34.5 mutant induced much higher IFN-β production than HSV-1 WT (Figure 5B), we measured the lytic replication of HSV-1 Δ34.5 mutant in cGAS-deficient L929 cells complemented with wild type cGAS or the S291A cGAS mutant up to 72 hours post-infection (Figure S5D). We observed that HSV-1 Δ34.5 mutant production was more apparently reduced in the S291A cGAS mutant cell line compared to wild type. However, VSV replicated at similar levels irrespective of cGAS WT or S291A mutant expression (Figure 6B). Furthermore, when myr-Akt1 was expressed in L929 cGAS−/− cells complemented with vector or mouse cGAS WT, L929 cells co-expressing cGAS and myr-Akt1 had a higher viral titer compared to cells expressing cGAS alone (Figure 6C). On the other hand, myr-Akt1 expression showed no effect on viral production in L929 cGAS−/− cells complemented with vector alone (Figure 6C). In summary, these data collectively indicate that expression of the Akt phosphorylation-resistant cGAS S291A leads to the augmented production of anti-viral IFN-β cytokine and the enhanced inhibition of HSV-1 replication, whereas expression of the constitutively active Akt1 attenuates the ability of cGAS to restrict DNA viral replication.

DISCUSSION

Our study identifies a mechanism for Akt kinase-mediated negative regulation of the cGAS signaling pathway, which potentially contributes to host health by dampening a prolonged immune response against pathogens. Importantly, failure to regulate cGAS activity may lead to excess immune response and inflammatory diseases. We showed that expression of Akt1 repressed cGAS-mediated cytokine production in L929 cells carrying cGAS WT, but not in L929 cells carrying the phosphorylation-resistant mutant cGAS S291A, whereas treatment with Akt inhibitor enhanced cytokine production and anti-viral response upon infection with DNA viruses as well as DNA stimulation suggesting that Akt functions as a direct repressor of cGAS.

Our data unambiguously show that the Akt-mediated phosphorylation of cGAS represses IFN-β production, whereas a phosphorylation-resistant cGAS mutant enhances IFN-β production, indicating that Akt1 is a negative regulator of cGAS-mediated IFN-β production and anti-viral immune response (Figure 6D). However, this model opposes other published observations that the activation of the phosphatidylinositol 3-kinase (PI3K)/Akt pathway is required for the full induction of IFN-stimulating genes (ISGs) (Kaur et al., 2008a; Kaur et al., 2008b). Specifically, it was shown that VSV infection induces Akt phosphorylation as a part of the host anti-viral response and activation of PI3K, and Akt is required for the full

activation and phosphorylation of IRF3 induced by TLR3 and TLR4 agonists (Schabbauer et al., 2008). Besides TLR stimulation, influenza virus infection also activates PI3K and Akt through a RIG-I-dependent signaling pathway that promotes IRF3 activation and type 1 IFN expression (Hrincius et al., 2011). In contrast, we showed Akt kinase was activated upon HSV-1 infection resulting in cGAS phosphorylation and ultimately, leading to decreased IFN-β production (Figures 4A, S3A and S5B). We also determined that the MVA robustly increased IFN-β in phosphorylation-resistant mutant cGAS S291 cells compared to cGAS WT cells. In addition, the PI3K/Akt pathway is activated at the early stage of vaccinia virus infection (Soares et al., 2009) and in some cases, activation of the Akt pathway by viral infection has a central role in viral replication and virus-induced apoptosis (Dunn and Connor, 2012). Therefore, at least some DNA viruses may have evolutionarily adjusted Akt-mediated cGAS regulation for their own needs in viral replication as well as for dampening the host innate immune response. On the other hand, while previous studies suggest an important role of Akt in anti-viral response, they have mostly shown the activation of Akt activity upon viral infection but failed to demonstrate specific roles of activated Akt in downstream anti-viral pathways. In fact, since Akt is phosphorylated and activated by TBK1 (Ou et al., 2011), it is possible that activated Akt suppresses the early step of PRR pathway as a feedback inhibition rather than stimulating a downstream step of PRR pathway. While we show that Akt phosphorylates cGAS and dampens its enzymatic activity, it remains to be determined what portion of cGAS is phosphorylated by Akt under steady state or in the context of viral infection. Thus, further study is needed to dissect the positive or negative role of Akt in anti-viral immune response upon RNA or DNA viral infection. Nevertheless, we show that Akt fine-tunes the IFN-mediated anti-viral pathway to ultimately ensure that the host DNA sensing innate immune response is kept in balance after responding to various stimuli such as DNA virus infections.

The DNA sensor cGAS detects cytosolic DNA species without a preference for self or non-self DNAs, implying that the DNA sensor-STING pathway might recognize endogenous DNA species that have localized to the cytosol. In agreement with this, several reports have demonstrated that the immunogenicity arising from cellular damage may be due to cGAS-induced sensing of endogenous DNA species and subsequent immune response (Deng et al., 2014; Hartlova et al., 2015; Woo et al., 2014) and that endogenous triggering by TREX1 deficiency robustly induces cell-autonomous immune response (Ablasser et al., 2014). Thus, cells should be able to actively regulate DNA sensing mechanism from being continuously stimulated by endogenous DNA, such as during cell division when self-DNA is exposed in the cytosol due to nuclear envelope collapse. The first hypothesis is that a DNA sensor is post-translationally modified in actively growing cells. In the second hypothesis, a DNA sensor might require another co-factor to specifically recognize non-self DNAs or a negative regulator exists to avoid self-DNA recognition. The present work supports the first hypothesis: Akt negatively regulates a primary DNA sensor cGAS activity by phosphorylating a specific serine residue localized in its catalytic region, resulting in the suppression of cGAMP synthesis. While it is clear that Akt attenuates the excessive activation of cGAS in response to DNA exposure, it is intriguing to ask why growth factor-induced Akt kinase, among numerous serine/threonine kinase candidates, modulates cGAS activity. We speculate that growth factors induce cell division by activating Akt and the

activated Akt subsequently regulates cGAS activity, preventing the unwanted recognition of self-DNA. Thus, it is important to better understand how DNA sensors such as cGAS and IFI16 or a safeguard of DNA sensing such as TREX1 are regulated to avoid the excessive response to the triggers of endogenous DNA.

It has been proposed that there are functional and structural similarities between oligoadenylate synthase (OAS) proteins and cGAS (Hornung et al., 2014). Indeed, the OAS proteins and cGAS are template-independent nucleotidyltransferases that, once activated by double-stranded nucleic acids in the cytosol, produce unique classes of 2'–5'-linked second messenger molecules, which - through distinct mechanisms - have crucial antiviral functions. OASs limit viral propagation through the activation of the enzyme RNase L, which degrades host and viral RNA. 2'–5'-linked cGAMP activates downstream signaling pathways to induce *de novo* antiviral gene expression (Hornung et al., 2014). Surprisingly, the predicted Akt target sequence in OAS1 is also localized in the catalytically critical region similar to cGAS (Figure S1C). This suggests that Akt-mediated phosphorylation is a common regulatory mechanism of the OAS family of cytosolic nucleic acid sensors. Further work is required with respect to the Akt-mediated regulation of the cGAS–STING and potentially OAS-RNAse L pathways, as their abnormal signaling can initiate a self-perpetuating inflammatory response. Regulating Akt activity may be a potential therapeutic strategy for manipulating the PRR-mediated anti-viral immune response.

EXPERIMENTAL PROCEDURES

Reagents, constructs and cell culture

The reagents were purchased from the following companies; Herring Testes (HT)-DNA, and anti-FlagM2-agarose beads (Sigma); Akt1/2 selective inhibitor VIII (EMD); ISD, Poly I:C (Invivogen); cGAMP (Biolog, Germany). Plasmids were purchased from Addgene (Myr-Akt1, Myr-Akt2, Myr-Akt3, Myr-Akt1 KD). To clone mouse cGAS, we purchased an expressing plasmid (GeneCopoeia, Inc.). Mouse cGAS-Flag constructs were created by subcloning the PCR products into pER-IRES-puromycin. Mutagenesis by overlap extension PCR was used to create human cGAS S305A or mouse cGAS S291A and the genes were subcloned into pER-IRES-puro. The constructs were sequenced by Genewiz and were identical to reference cGAS sequences except for the defined mutations. HEK293T, RAW 264.7, L929 wild type, L929 cGAS knockout (Gao et al., 2013a), and Vero cells were cultured in Dulbecco's modified Eagle's medium (DMEM; Gibco-BRL) containing 4 mM glutamine and 10% FBS. THP1-Lucia™ ISG cells express the secreted luciferase (Lucia) reporter gene under the control of an IRF-inducible promoter comprising of five IFN-stimulated response elements (ISRE) fused to an ISG54 minimal promoter. Transient transfections were performed with Lipofectamine 2000 (Invitrogen), or calcium phosphate (Clontech), according to the manufacturer’s instructions. Stably expressing cell lines of vector alone, cGAS, or Akt in L929 cGAS−/− cells were generated using a standard selection protocol with 2 μg/ml of puromycin or 500 μg/ml of G418.

Mass spectrometry

HEK293T cells were collected 48 h after transfection with cGAS-Flag, and lysed with NP-40 buffer [50 mM HEPES, pH 7.4, 150 mM NaCl, 1 mM EDTA, 1% (vol/vol) NP-40] supplemented with complete protease inhibitor cocktail (Roche) and Ser/Thr-phosphatase inhibitor cocktail (Sigma). Post centrifugation, supernatants were mixed with a 50% slurry of Flag M2 beads (Sigma), and the binding reaction mix was incubated for 4 h at 4°C. Precipitates were washed extensively with lysis buffer. Proteins bound to Flag M2 beads were eluted and separated in a NuPAGE 4 to 12% Bis-Tris gradient gel (Invitrogen). Following Coomassie brilliant blue staining, protein bands corresponding to the expected size of cGAS-Flag were excised and separately analyzed by ion-trap mass spectrometry at the Harvard Taplin Biological Mass Spectrometry Facility (Boston, MA).

Dual luciferase assay

HEK293T cells were seeded into twelve-well plates. 24 h later, the cells were transiently transfected with 100 ng of IFN-β luciferase reporter plasmid and 20 ng of TK-renilla luciferase. In addition, 100 ng of plasmid encoding human or mouse cGAS, 50 ng of plasmid encoding STING, or 400 ng myr-Akt was transfected as indicated in Figure 2B. 48 h after transfection, whole-cell lysates were prepared and subjected to the Dual-Glo luciferase assay according to manufacturer's instructions (Promega). Results are presented with renilla luciferase levels normalized by the firefly luciferase levels.

Immunoblot and immunoprecipitation

Cell lysates were collected in 1% NP-40 buffer and quantified by BCA protein assay (Thermo Scientific). Proteins were separated by SDS-PAGE and transferred to PVDF membrane (Bio-Rad) by semi-dry transfer at 25V for 40 minutes. All membranes were blocked in 5% milk in Tris-Buffered Saline (TBST) and probed overnight with indicated antibodies, which are diluted in the blocking buffer solution at 4°C. Primary antibodies included: mouse Flag (Sigma), rabbit V5 (Bethyl Laboratories), rabbit HA (Covance), mouse panAkt (Cell Signaling). HRP-conjugated secondary antibodies were incubated on membranes in 5% milk in TBST and bands were developed with ECL reagent (Thermo Scientific) and imaged using a Fuji LAS-4000 imager.

For immunoprecipitation, cells were harvested and then lysed in 1% NP-40 buffer supplemented with a complete protease inhibitor cocktail (Roche). After pre-clearing with protein A/G agarose beads for 1 h at 4°C, whole cell lysates were used for immunoprecipitation with the indicated antibodies. 30 μl of Flag M2 beads (Sigma) was added to 1 ml of cell lysates and incubated at 4°C for 4 h. Immunoprecipitates were extensively washed 5 times with lysis buffer and eluted with SDS loading buffer by boiling for 5 min.

Protein purification

Mouse MBP-cGAS fusion protein (aa151–522) was expressed in BL21 (DE3, RIPL strain. *E. coli*) and were grown at 37°C until reaching OD_{600} = 0.6. The temperature was then shifted to 18°C and grown overnight after adding 1mM IPTG. Cel ls were collected by

centrifugation and lysed with 1% NP40 buffer. Clarified lysates were mixed with Ni-NTA agarose (Invitrogen) and washed 5 times with lysis buffer prior to elution of protein using 150mM imidazole. The concentrated protein was aliquotted and stored at −80 °C for the in vitro cGAS enzyme assay.

The purification of mouse cGAS protein including the unnatural amino acid was described previously (Shi et al., 2014). Briefly, the Ser291 (AGC) codon was replaced by the pSer291 (UAG) amber codon by site-directed mutagenesis (Stratagene). The plasmid expressing cGAS-291(UAG) and $tRNA^{Sep}$ was transformed into *E. coli* BL21ΔSerB containing pKD-SepRS-EF-Sep and E. *coli* were grown at 25 °C for autoinduction, supplemented with solution including 100 μg ml^{-1} of Amp, 50 μg ml^{-1} Kan, 12 μg ml^{-1} Tet, 2 mM Sep, 5,052 solution and phosphate buffer. After induction, *E. coli* was harvested, lysed, subjected to Ni^{2}+NTA agarose column and anion exchange column purification. Finally, purified proteins were separated by 10% SDS–PAGE and stained with Coomassie brilliant blue.

In vitro Akt kinase assay

The *in vitro* kinase assays using MBP-cGAS and GSK as substrates were performed using a non-radioactive assay (Cell Signaling Technology). Briefly, the immunoprecipitated phosho-Akt were used in a kinase reaction with 1 μg MBP-cGAS WT or S291A, or GSK as substrates in the presence of 100 μM ATP in a kinase assay buffer [25 mM Tris pH 7.5, 5 mM β-glycerophosphate, 2 mM DTT, 0.1 mM Na_3VO_4, 10 mM $MgCl_2$] and a serine/threonine phosphatase inhibitor cocktail (Sigma). The kinase reaction was performed at 30°C for 35 minutes and the end products were resolved on 10% SDS-PAGE gel followed by immunoblotting with the indicated antibodies.

In vitro cGAS activity assay

For *in vitro* cGAS enzymatic reactions, 1μM MBP-cGAS or MBP-cGAS variant was mixed with 250μM GTP and 10μCi P^{32} α phosphate radiolabed ATP in buffer [20mM Tris-Cl (pH 7.5), 150mM NaCl, 5mM $MgCl_2$, 1mM DTT]. After a 1hr incubation at 37°C, the rea ction was treated with 5 units of alkaline phosphatase (Roche) for 30 minutes to stop the reaction and 1μl of reaction solution was spotted onto TLC plates (HPTLC silica gel 60 F254, 20×10 cm) with the solvent 1:1.5 [v/v] 1M $(NH4)_2SO_4$ and 1.5M KH_2PO_4. To visualize the reaction, the TLC plates were air-dried and imaged using a Fuji Phosphor Imager.

RNA extraction and real-time PCR

Total RNA was isolated from cells with TriReagent (Sigma). cDNA synthesis was performed using the iScript cDNA Synthesis kit (Bio-Rad), and qPCR reaction was monitored with SYBR Green Supermix (Bio-Rad).

Enzyme-linked Immunosorbant Assay (ELISA)

L929 cells were treated with HT-DNA for 18 hours and the cell culture supernatant was collected and measured for IFN-β production by sandwich ELISA using a mouse IFN-β ELISA kit (PBL Biomedical Laboratories) according to the manufacturer's protocols.

Viral plaque assays

HSV-1 strain F strain and HSV ΔICP34.5 (Liang et al., 2014) were grown in Vero cells propagated in DMEM supplemented with 10% FBS and antibiotics. L929 cells were inoculated with virus in DMEM supplemented with 2% FBS for 1h. After incubation for indicated times (0h, 10h, 24h, 48h, 72 h), culture medium were harvested and the viral titer was determined. Briefly, culture medium from L929 cells were serially diluted in DMEM supplemented with 10% FBS and used to infect 80% confluent monolayers of Vero cells growing in 6-well plates. After infection, the monolayers were rinsed and overlaid with 7% methylcelluose. Plaques were counted after 3 to 5 days.

cGAMP bio-assay

L929 cells treated with HT-DNA or Akt inhibitor for 9 hours were trypsinized and washed with PBS. Freezing and thawing after storage at −80 °C l ysed the pelleted cells. Cell extracts were incubated with Benzonase and heat-treated as previously reported (Wu et al., 2013). IRF responsive THP-1 ISG54-Lucia cells (Invivogen) were cultured in RPMI-1640 supplemented with 10% FBS and antibiotics. Samples of cell lysates were mixed with a digitonin permeabilization solution (50mM HEPES pH 7.0. 100 mM KCl, 3 mM $MgCl_2$, 0.1 mM DTT, 85 mM Sucrose, 0.2% BSA, 1mM ATP, 10 μg/ml Digitonin). The mixtures were incubated for 30 minutes at 37 °C in microcentrifuge tubes. The prec ipitated cells were dissolved in RPMI complete medium and incubated for 18 hours before luciferase measurement. Whole-cell lysates were prepared and subjected to the Renilla luciferase assay reagent according to manufacturer's instructions (Promega). cGAMP was used as a standard.

Statistical Analysis

All data were analyzed using a two-tailed Student's t test with a minimum of n=3. p-values less than 0.05 were considered significant. *p<0.05, **p<0.005.

Supplementary Material

Refer to Web version on PubMed Central for supplementary material.

ACKNOWLEDGMENTS

This work was partly supported by CA82057, CA91819, CA31363, CA115284, CA147868, CA148616, DE019085, AI073099, Hastings Foundation, Fletcher Jones Foundation, GRL Program (K20815000001) from National Research Foundation of Korea (JUJ), and grants 2011-0020322 and KAIST Future Systems Healthcare Project (H-SP). We thank Drs. James Chen, Fanxiu Zhu, and Michaela Gack for providing cGAS −/− L929 cells, THP1-Lucia™ ISG cells, and viruses, respectively, and all Jung's laboratory members for their discussions.

REFERENCES

Ablasser A, Bauernfeind F, Hartmann G, Latz E, Fitzgerald KA, Hornung V. RIG-I-dependent sensing of poly(dA:dT) through the induction of an RNA polymerase III-transcribed RNA intermediate. Nature immunology. 2009; 10:1065–1072. [PubMed: 19609254]

Ablasser A, Goldeck M, Cavlar T, Deimling T, Witte G, Rohl I, Hopfner KP, Ludwig J, Hornung V. cGAS produces a 2'–5'-linked cyclic dinucleotide second messenger that activates STING. Nature. 2013; 498:380–384. [PubMed: 23722158]

Ablasser A, Hemmerling I, Schmid-Burgk JL, Behrendt R, Roers A, Hornung V. TREX1 deficiency triggers cell-autonomous immunity in a cGAS-dependent manner. Journal of immunology. 2014; 192:5993–5997.

Bhat N, Fitzgerald KA. Recognition of cytosolic DNA by cGAS and other STING-dependent sensors. European journal of immunology. 2014; 44:634–640. [PubMed: 24356864]

Chiu YH, Macmillan JB, Chen ZJ. RNA polymerase III detects cytosolic DNA and induces type I interferons through the RIG-I pathway. Cell. 2009; 138:576–591. [PubMed: 19631370]

Deng L, Liang H, Xu M, Yang X, Burnette B, Arina A, Li XD, Mauceri H, Beckett M, Darga T, et al. STING-Dependent Cytosolic DNA Sensing Promotes Radiation-Induced Type I Interferon-Dependent Antitumor Immunity in Immunogenic Tumors. Immunity. 2014; 41:843–852. [PubMed: 25517616]

Dunn EF, Connor JH. HijAkt: The PI3K/Akt pathway in virus replication and pathogenesis. Progress in molecular biology and translational science. 2012; 106:223–250. [PubMed: 22340720]

Elinav E, Strowig T, Henao-Mejia J, Flavell RA. Regulation of the antimicrobial response by NLR proteins. Immunity. 2011; 34:665–679. [PubMed: 21616436]

Ferguson BJ, Mansur DS, Peters NE, Ren H, Smith GL. DNA-PK is a DNA sensor for IRF–3-dependent innate immunity. eLife. 2012; 1:e00047. [PubMed: 23251783]

Fernandes-Alnemri T, Yu JW, Datta P, Wu J, Alnemri ES. AIM2 activates the inflammasome and cell death in response to cytoplasmic DNA. Nature. 2009; 458:509–513. [PubMed: 19158676]

Gao D, Wu J, Wu YT, Du F, Aroh C, Yan N, Sun L, Chen ZJ. Cyclic GMP-AMP synthase is an innate immune sensor of HIV and other retroviruses. Science. 2013a; 341:903–906. [PubMed: 23929945]

Gao P, Ascano M, Wu Y, Barchet W, Gaffney BL, Zillinger T, Serganov AA, Liu Y, Jones RA, Hartmann G, et al. Cyclic [G(2',5')pA(3',5')p] is the metazoan second messenger produced by DNA-activated cyclic GMP-AMP synthase. Cell. 2013b; 153:1094–1107. [PubMed: 23647843]

Hartlova A, Erttmann SF, Raffi FA, Schmalz AM, Resch U, Anugula S, Lienenklaus S, Nilsson LM, Kroger A, Nilsson JA, et al. DNA Damage Primes the Type I Interferon System via the Cytosolic DNA Sensor STING to Promote Anti-Microbial Innate Immunity. Immunity. 2015; 42:332–343. [PubMed: 25692705]

Hornung V, Ablasser A, Charrel-Dennis M, Bauernfeind F, Horvath G, Caffrey DR, Latz E, Fitzgerald KA. AIM2 recognizes cytosolic dsDNA and forms a caspase-1-activating inflammasome with ASC. Nature. 2009; 458:514–518. [PubMed: 19158675]

Hornung V, Hartmann R, Ablasser A, Hopfner KP. OAS proteins and cGAS: unifying concepts in sensing and responding to cytosolic nucleic acids. Nature reviews Immunology. 2014:521–528.

Hrincius ER, Dierkes R, Anhlan D, Wixler V, Ludwig S, Ehrhardt C. Phosphatidylinositol-3-kinase (PI3K) is activated by influenza virus vRNA via the pathogen pattern receptor Rig-I to promote efficient type I interferon production. Cellular microbiology. 2011; 13:1907–1919. [PubMed: 21899695]

Kanai R, Zaupa C, Sgubin D, Antoszczyk SJ, Martuza RL, Wakimoto H, Rabkin SD. Effect of gamma34.5 deletions on oncolytic herpes simplex virus activity in brain tumors. Journal of virology. 2012; 86:4420–4431. [PubMed: 22345479]

Kaur S, Sassano A, Dolniak B, Joshi S, Majchrzak-Kita B, Baker DP, Hay N, Fish EN, Platanias LC. Role of the Akt pathway in mRNA translation of interferon-stimulated genes. Proc Natl Acad Sci U S A. 2008a; 105:4808–4813. [PubMed: 18339807]

Kaur S, Sassano A, Joseph AM, Majchrzak-Kita B, Eklund EA, Verma A, Brachmann SM, Fish EN, Platanias LC. Dual regulatory roles of phosphatidylinositol 3-kinase in IFN signaling. Journal of immunology. 2008b; 181:7316–7323.

Kawai T, Akira S. Toll-like receptors and their crosstalk with other innate receptors in infection and immunity. Immunity. 2011; 34:637–650. [PubMed: 21616434]

Kranzusch PJ, Lee AS, Berger JM, Doudna JA. Structure of human cGAS reveals a conserved family of second-messenger enzymes in innate immunity. Cell reports. 2013; 3:1362–1368. [PubMed: 23707061]

Latz E. The inflammasomes: mechanisms of activation and function. Current opinion in immunology. 2010; 22:28–33. [PubMed: 20060699]

Lee S, Oh S, Yang A, Kim J, Soll D, Lee D, Park HS. A facile strategy for selective incorporation of phosphoserine into histones. Angew Chem Int Ed Engl. 2013; 52:5771–5775. [PubMed: 23533151]

Li XD, Wu J, Gao D, Wang H, Sun L, Chen ZJ. Pivotal roles of cGAS-cGAMP signaling in antiviral defense and immune adjuvant effects. Science. 2013; 341:1390–1394. [PubMed: 23989956]

Li Y, Zhang C, Chen X, Yu J, Wang Y, Yang Y, Du M, Jin H, Ma Y, He B, et al. ICP34.5 protein of herpes simplex virus facilitates the initiation of protein translation by bridging eukaryotic initiation factor 2alpha (eIF2alpha) and protein phosphatase 1. The Journal of biological chemistry. 2011; 286:24785–24792. [PubMed: 21622569]

Liang Q, Seo GJ, Choi YJ, Kwak MJ, Ge J, Rodgers MA, Shi M, Leslie BJ, Hopfner KP, Ha T, et al. Crosstalk between the cGAS DNA sensor and Beclin-1 autophagy protein shapes innate antimicrobial immune responses. Cell host & microbe. 2014; 15:228–238. [PubMed: 24528868]

Liu Y, Jesus AA, Marrero B, Yang D, Ramsey SE, Montealegre Sanchez GA, Tenbrock K, Wittkowski H, Jones OY, Kuehn HS, et al. Activated STING in a vascular and pulmonary syndrome. The New England journal of medicine. 2014; 371:507–518. [PubMed: 25029335]

Manning BD, Cantley LC. AKT/PKB signaling: navigating downstream. Cell. 2007; 129:1261–1274. [PubMed: 17604717]

Medzhitov R, Janeway C Jr. The Toll receptor family and microbial recognition. Trends in microbiology. 2000; 8:452–456. [PubMed: 11044679]

Munz C, Lunemann JD, Getts MT, Miller SD. Antiviral immune responses: triggers of or triggered by autoimmunity? Nature reviews Immunology. 2009; 9:246–258.

Orvedahl A, Alexander D, Talloczy Z, Sun Q, Wei Y, Zhang W, Burns D, Leib DA, Levine B. HSV-1 ICP34.5 confers neurovirulence by targeting the Beclin 1 autophagy protein. Cell host & microbe. 2007; 1:23–35. [PubMed: 18005679]

Ou YH, Torres M, Ram R, Formstecher E, Roland C, Cheng T, Brekken R, Wurz R, Tasker A, Polverino T, et al. TBK1 directly engages Akt/PKB survival signaling to support oncogenic transformation. Molecular cell. 2011; 41:458–470. [PubMed: 21329883]

Paludan SR, Bowie AG. Immune sensing of DNA. Immunity. 2013; 38:870–880. [PubMed: 23706668]

Park HS, Hohn MJ, Umehara T, Guo LT, Osborne EM, Benner J, Noren CJ, Rinehart J, Soll D. Expanding the genetic code of Escherichia coli with phosphoserine. Science. 2011; 333:1151–1154. [PubMed: 21868676]

Roberts TL, Idris A, Dunn JA, Kelly GM, Burnton CM, Hodgson S, Hardy LL, Garceau V, Sweet MJ, Ross IL, et al. HIN-200 proteins regulate caspase activation in response to foreign cytoplasmic DNA. Science. 2009; 323:1057–1060. [PubMed: 19131592]

Schabbauer G, Luyendyk J, Crozat K, Jiang Z, Mackman N, Bahram S, Georgel P. TLR4/CD14-mediated PI3K activation is an essential component of interferon-dependent VSV resistance in macrophages. Molecular immunology. 2008; 45:2790–2796. [PubMed: 18339426]

Shi M, Cho H, Inn KS, Yang A, Zhao Z, Liang Q, Versteeg GA, Amini-Bavil-Olyaee S, Wong LY, Zlokovic BV, et al. Negative regulation of NF-kappaB activity by brain-specific TRIpartite Motif protein 9. Nature communications. 2014; 5:4820.

Soares JA, Leite FG, Andrade LG, Torres AA, De Sousa LP, Barcelos LS, Teixeira MM, Ferreira PC, Kroon EG, Souto-Padron T, et al. Activation of the PI3K/Akt pathway early during vaccinia and cowpox virus infections is required for both host survival and viral replication. Journal of virology. 2009; 83:6883–6899. [PubMed: 19386722]

Sun L, Wu J, Du F, Chen X, Chen ZJ. Cyclic GMP-AMP synthase is a cytosolic DNA sensor that activates the type I interferon pathway. Science. 2013; 339:786–791. [PubMed: 23258413]

Takaoka A, Wang Z, Choi MK, Yanai H, Negishi H, Ban T, Lu Y, Miyagishi M, Kodama T, Honda K, et al. DAI (DLM-1/ZBP1) is a cytosolic DNA sensor and an activator of innate immune response. Nature. 2007; 448:501–505. [PubMed: 17618271]

Unterholzner L, Keating SE, Baran M, Horan KA, Jensen SB, Sharma S, Sirois CM, Jin T, Latz E, Xiao TS, et al. IFI16 is an innate immune sensor for intracellular DNA. Nature immunology. 2010; 11:997–1004. [PubMed: 20890285]

Woo SR, Fuertes MB, Corrales L, Spranger S, Furdyna MJ, Leung MY, Duggan R, Wang Y, Barber GN, Fitzgerald KA, et al. STING-dependent cytosolic DNA sensing mediates innate immune recognition of immunogenic tumors. Immunity. 2014; 41:830–842. [PubMed: 25517615]

Wu J, Sun L, Chen X, Du F, Shi H, Chen C, Chen ZJ. Cyclic GMP-AMP is an endogenous second messenger in innate immune signaling by cytosolic DNA. Science. 2013; 339:826–830. [PubMed: 23258412]

Zhang Z, Yuan B, Bao M, Lu N, Kim T, Liu YJ. The helicase DDX41 senses intracellular DNA mediated by the adaptor STING in dendritic cells. Nature immunology. 2011; 12:959–965. [PubMed: 21892174]

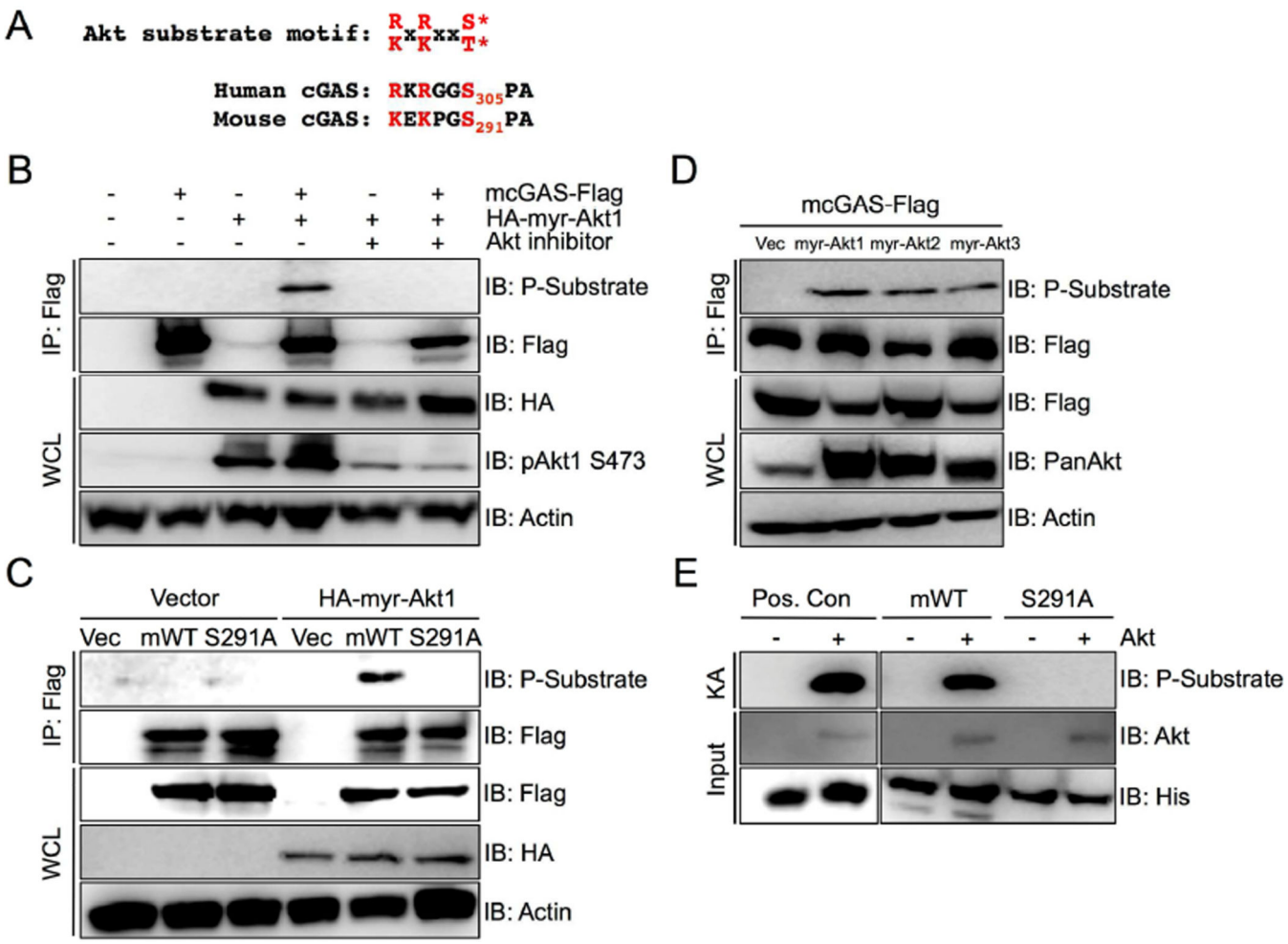

Figure 1. cGAS is an Akt substrate

(A) Sequence comparison of the phosphorylated peptides from human and mouse cGAS. Residues that support its identity as an Akt substrate motif are highlighted in red.

(B) Mouse cGAS-Flag (mcGAS-Flag) was immunoprecipitated with anti-Flag M2 beads from lysates of 293T cells transiently transfected with mcGAS-Flag, HA-myr-Akt1 or vector alone for 24 hours. Cells were treated for 8 hours with Akt1/2 selective inhibitor VIII (10μM). The immunoprecipitates were probed with Akt phosphosubstrate and Flag antibodies. Whole cell lysates (WCLs) were probed with antibodies recognizing active pAkt1 S473, HA, or Actin (loading control).

(C) 293T cells expressing vector alone or HA-myr-Akt1 were co-transfected with vector (Vec), mouse cGAS-Flag (mWT), or mouse cGAS-S291A-Flag (S291A) for 24 hours. cGAS-Flag immunoprecipitates were probed with Akt phosphosubstrate and Flag antibodies, and WCLs were probed with Flag, HA, or Actin (loading control) antibodies.

(D) Mouse cGAS-Flag was co-transfected with vector (Vec), myr-Akt1, myr-Akt2, or myr-Akt3 in 293T cells for 24 hours. cGAS-Flag immunoprecipitates were probed with the Akt phosphosubstrate and Flag antibodies and WCLs were probed with an Akt phosphosubstrate, Flag, Pan-Akt detecting all Akt isoforms, and Actin (loading control) antibodies.

(E) His-tagged C-terminal fragment of cGAS (aa161–522) WT or with the S291A mutation were used as substrates for *in vitro* kinase reactions for immmunoprecipitated active Akt1. His-Gsk protein, the known Akt substrate, is a positive control. Phosphorylation was detected with an Akt phosphosubstrate antibody. KA: Kinase Assay; Pos. Con: His-Gsk protein

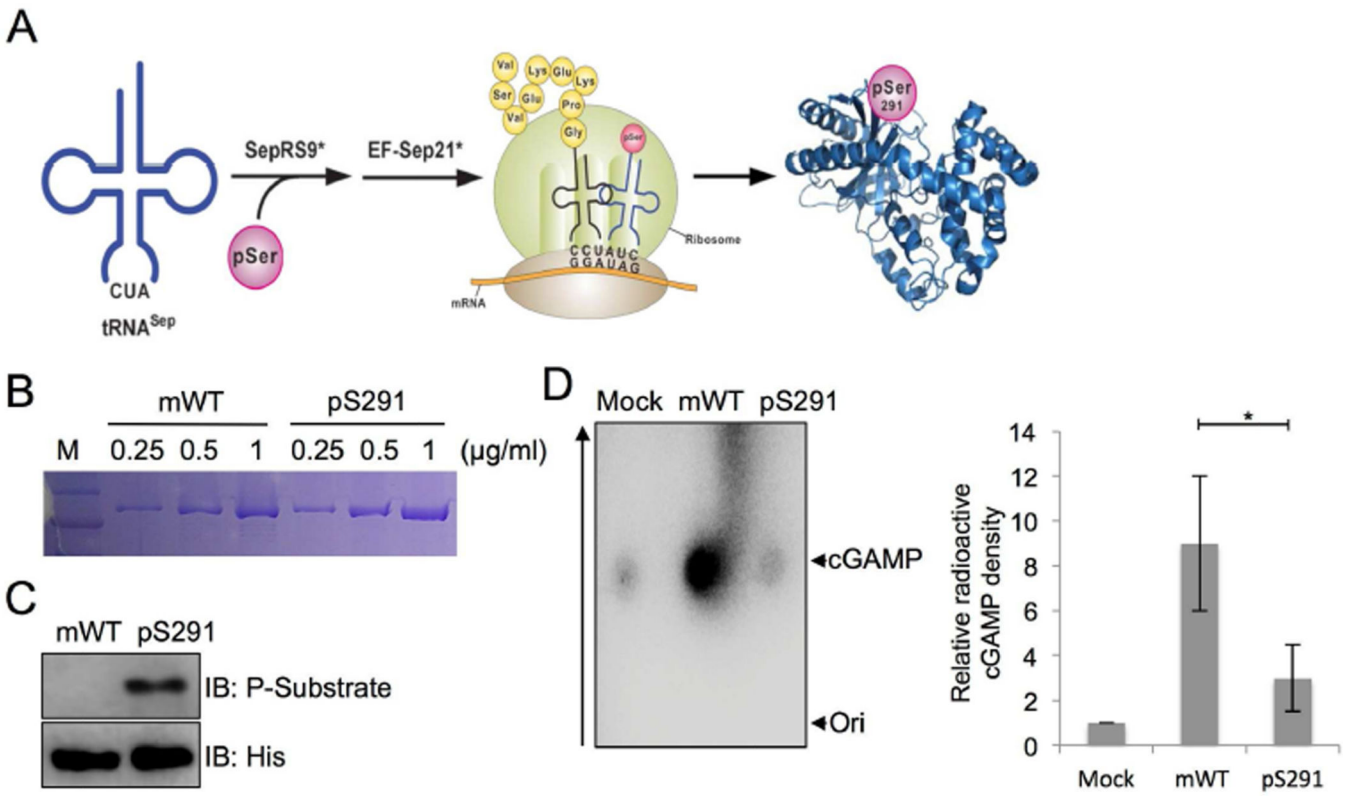

Figure 2. Phospho-cGAS has a negative role in its enzymatic activity

(A) A schematic describing site-specific serine 291 phosphorylation with a Sep-accepting transfer RNA ($tRNA^{Sep}$), its cognate phosphoseryl-tRNA synthetase (SepRS) and elongation factor-Tu (EF-Sep) in an engineered *E coli* BL21 strain.

(B) The purification of mouse cGAS WT (mWT) and cGAS pS291 (pS291) protein containing an unnatural pS291 amino acid for *in vitro* enzymatic assay. Amino acids 141–507 of mouse cGAS fused to MBP were purified from an engineered *E. coli* BL21 strain. Indicated amounts of purified proteins (μg/ml) were loaded and visualized by Coomassie brilliant blue staining.

(C) Mouse cGAS WT (mWT) and cGAS with the unnatural pS291 amino acid (pS291) were probed with Akt phosphosubstrate and His antibodies.

(D) *In vitro* enzymatic assays were performed in the presence of P^{32}-α-GTP with amino acids 141–507 of mouse cGAS (mWT) and the same fragment with the unnatural pS291 amino acid (pS291) purified from engineered *E. coli* BL21 strain. cGAMP production was analyzed by TLC and autoradiography. The bottom arrow shows the spotted origin and the top arrow shows the migrated cGAMP. A representative image was shown and the right panel shows the plot from triplicated experiments showing the relative radioactivity of P^{32}-labeled cGAMP normalized to the mock control.

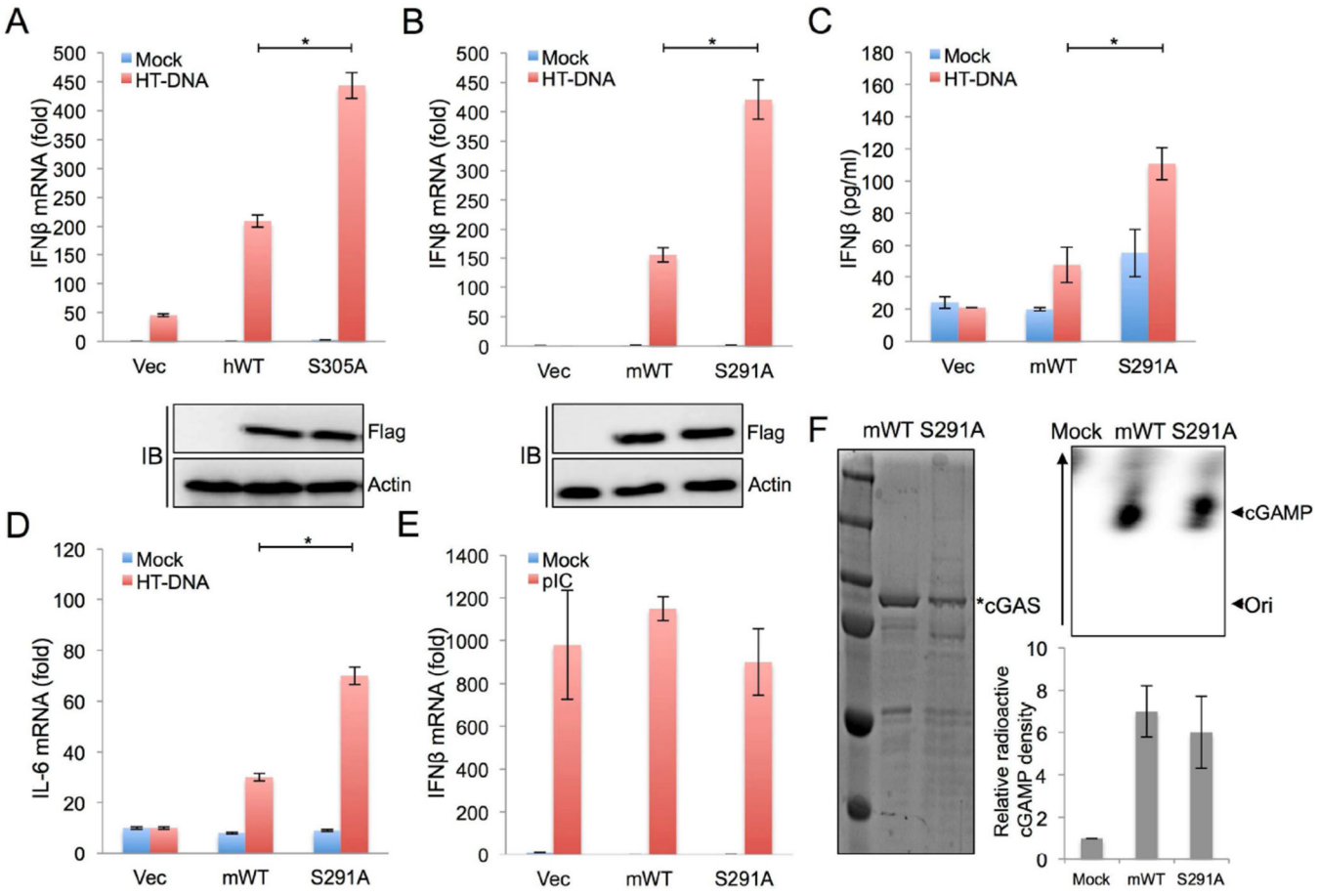

Figure 3. Serine phosphorylation regulates cGAS activity

(A) L929 cGAS−/− cells were stably complemented with empty vector, human cGAS WT (hWT), or human cGAS S305A (S305A). Those cell lines were stimulated with HT-DNA (2μg/ml) for 9 hours. The expression of IFN-β mRNA was measured by real-time PCR.

(B) L929 cGAS−/− cells were stably complemented with empty vector, mouse cGAS WT (mWT), or mouse cGAS S291A (S291A). Those cell lines were stimulated with HT-DNA (2μg/ml) for 9 hours. The expression of IFN-β mRNA was measured by real-time PCR.

(C) L929 cell lines used in (B) were stimulated with HT-DNA (2μg/ml) for 18 hours. The production of IFN-β was measured by ELISA.

(D) L929 cell lines used in (B) were stimulated with HT-DNA (2μg/ml) for 9 hours. The expression of IL-6 mRNA was measured by real-time PCR.

(E) L929 cell lines used in (B) were stimulated with poly I:C (1μg/ml) for 8 hours. The expression of IFN-β mRNA was measured by real-time PCR.

(F) *In vitro* enzymatic assays were performed in the presence of P^{32}-α-GTP with mouse cGAS (aa141–507) WT and cGAS S291A purified from *E. coli* (left panel). cGAMP production was analyzed by TLC and autoradiograph (top right panel). The bottom arrow shows the spotted origin and the top arrow shows the migrated cGAMP. A representative image was shown and the right bottom panel shows the plot from triplicated experiments showing the relative radioactivity of P^{32}-labeled cGAMP normalized to the mock control. * $p<0.05$

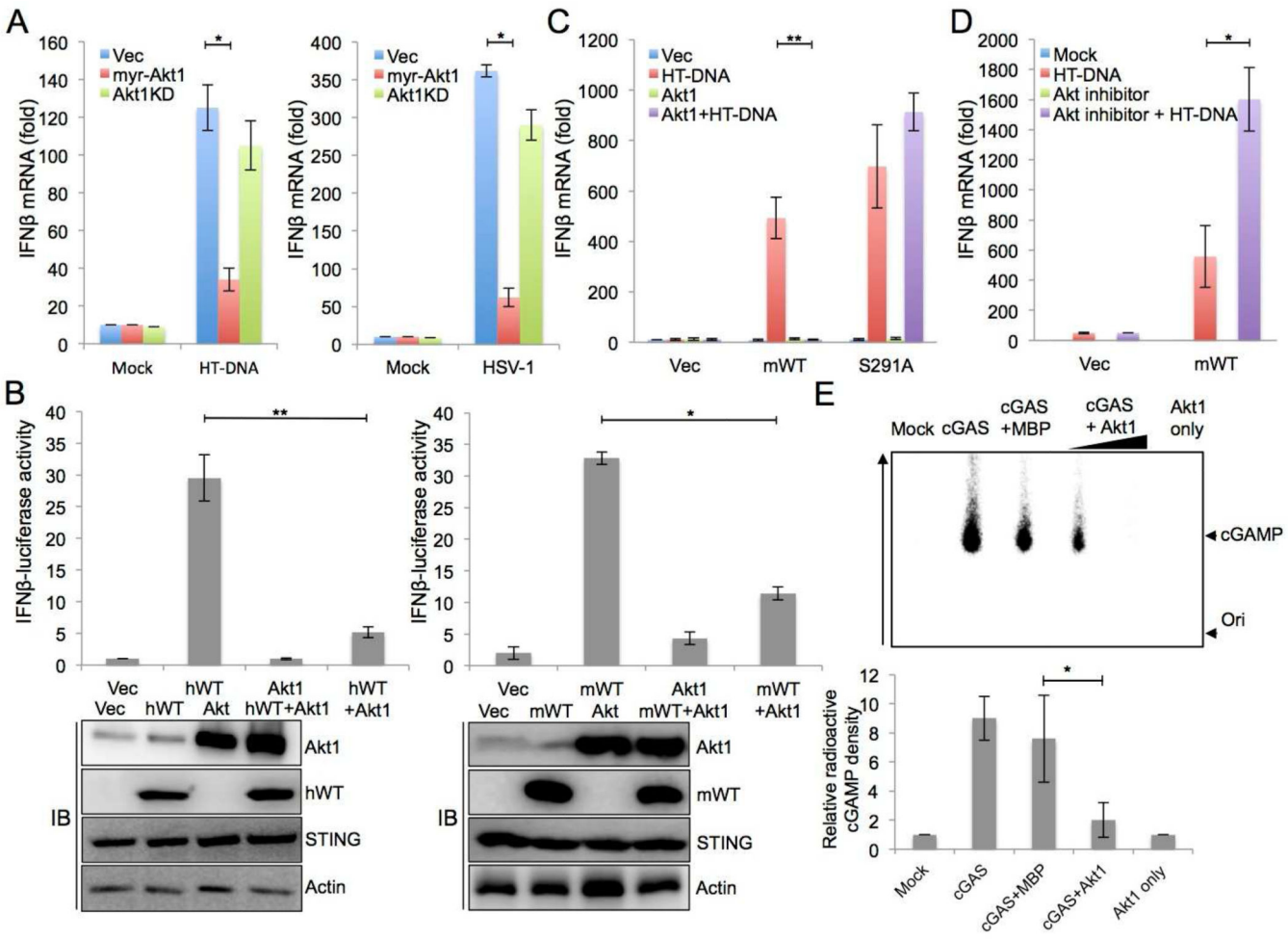

Figure 4. Akt1 negatively regulates cGAS-mediated cytokine production via cGAS phosphorylation at S291

(A) RAW 264.7 cells were electroporated with vector, myr-Akt1 or kinase dead Akt1 (Akt1 KD), respectively. At 48 h post transfection, cells were treated with HT-DNA stimulation (left panel) for 9 hours or infected with HSV-1 (right panel, moi = 10) for 12 hours. The expression of IFN-β mRNA was measured by real-time PCR.

(B) Akt1 suppression of cGAS-mediated IFN-β promoter activation. HEK293T cells were transfected with human (left panel) or mouse (right panel) cGAS together with empty vector or HA-myrAkt1. In addition, all samples were co-transfected with STING, IFN-β-Firefly luciferase, and TK-renilla luciferase. Reporter activity was measured at 16 h post-transfection.

(C) Mouse cGAS variant L929 cell lines were stably expressed with empty vector or myr-Akt1. The expression of IFN-β mRNA was measured by real-time PCR after HT-DNA stimulation (2μg/ml) for 9 hours.

(D) L929 cGAS−/− cells complemented with empty vector or mouse cGAS WT (mWT) were treated with 5μM Akt1/2 selective inhibitor VIII or DMSO vehicle and stimulated with HT-DNA (2μg/ml) for 9 hours. The expression of IFN-β mRNA was measured by real-time PCR.

(E) Mock or cGAS (aa141-aa507) WT purified from *E. coli* were incubated for 30 min with MBP or immunoprecipiated, active Akt1 in the presence of P^{32}-α-GTP. cGAMP production was analyzed by TLC and autoradiograph. The bottom arrow shows the spotted origin and the top arrow shows the migrated cGAMP. A representative image was shown and the bottom panel shows the plot from triplicated experiments showing the relative radioactivity of P^{32}-labeled cGAMP normalized to the mock control. *$p<0.05$, **$p<0.005$.

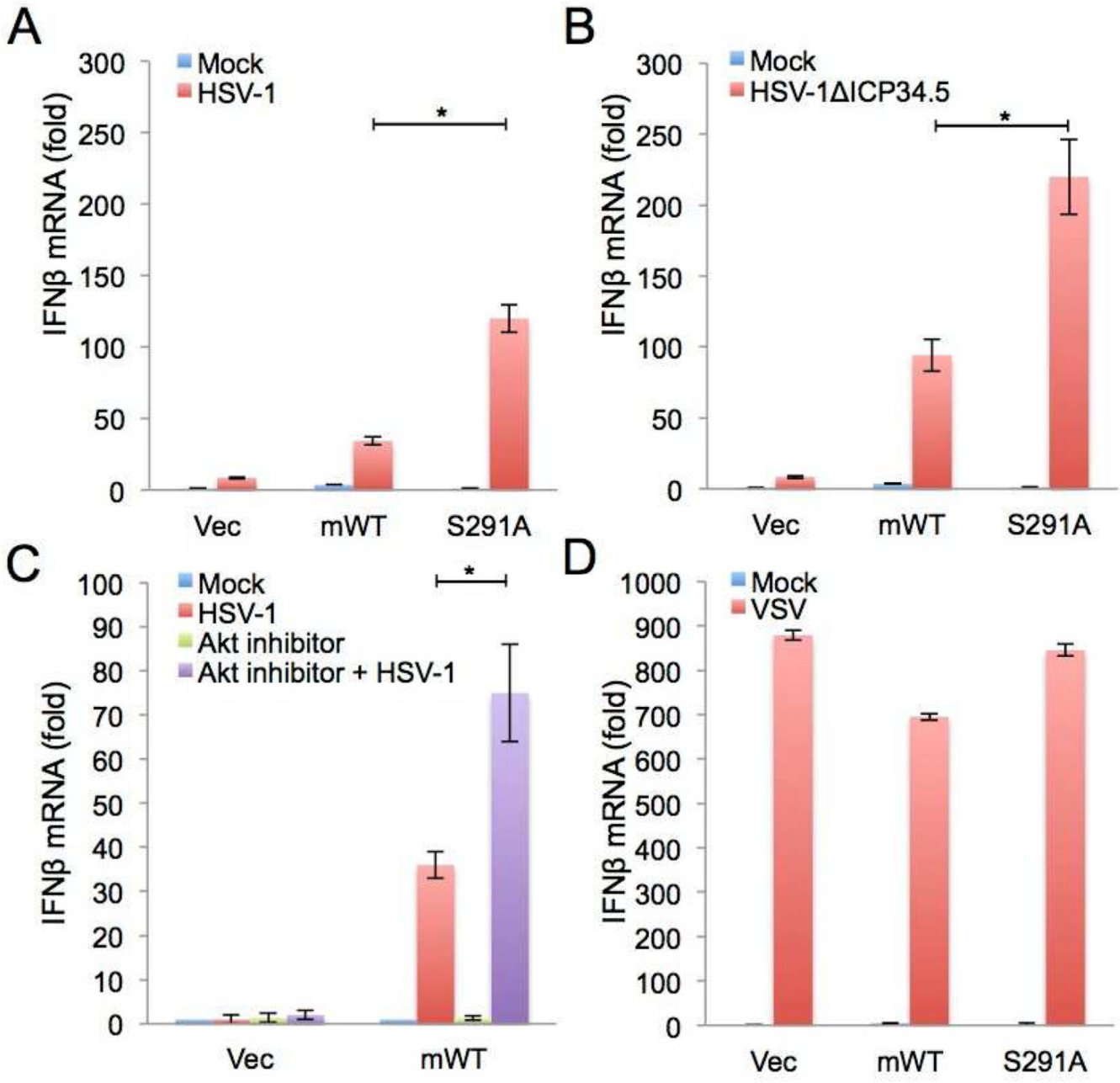

Figure 5. The negative regulation of cGAS by Akt upon virus infection

(A–B) L929 cGAS−/− cells were stably complemented with empty vector, mouse cGAS WT (mWT), or S291A. The expression of IFN-β mRNA was measured by real-time PCR after infection with HSV-1 WT (moi =5, A) or HSV-1 ICPΔ34.5 (moi = 5, B) for 12 hours. (C) L929 cGAS−/− cells complemented with empty vector or mouse cGAS WT (mWT) were treated with 5μM Akt1/2 selective inhibitor VIII or DMSO vehicle and infected with HSV-1 WT (moi = 5) for 12 hours. The expression of IFN-β mRNA was measured by real-time PCR.

(D) L929 cGAS−/− cells were stably complemented with empty vector, mouse cGAS WT (mWT) or S291A. The expression of IFN-β mRNA was measured by real-time PCR after infection with VSV (moi = 1) for 8 hours. * $p<0.05$.

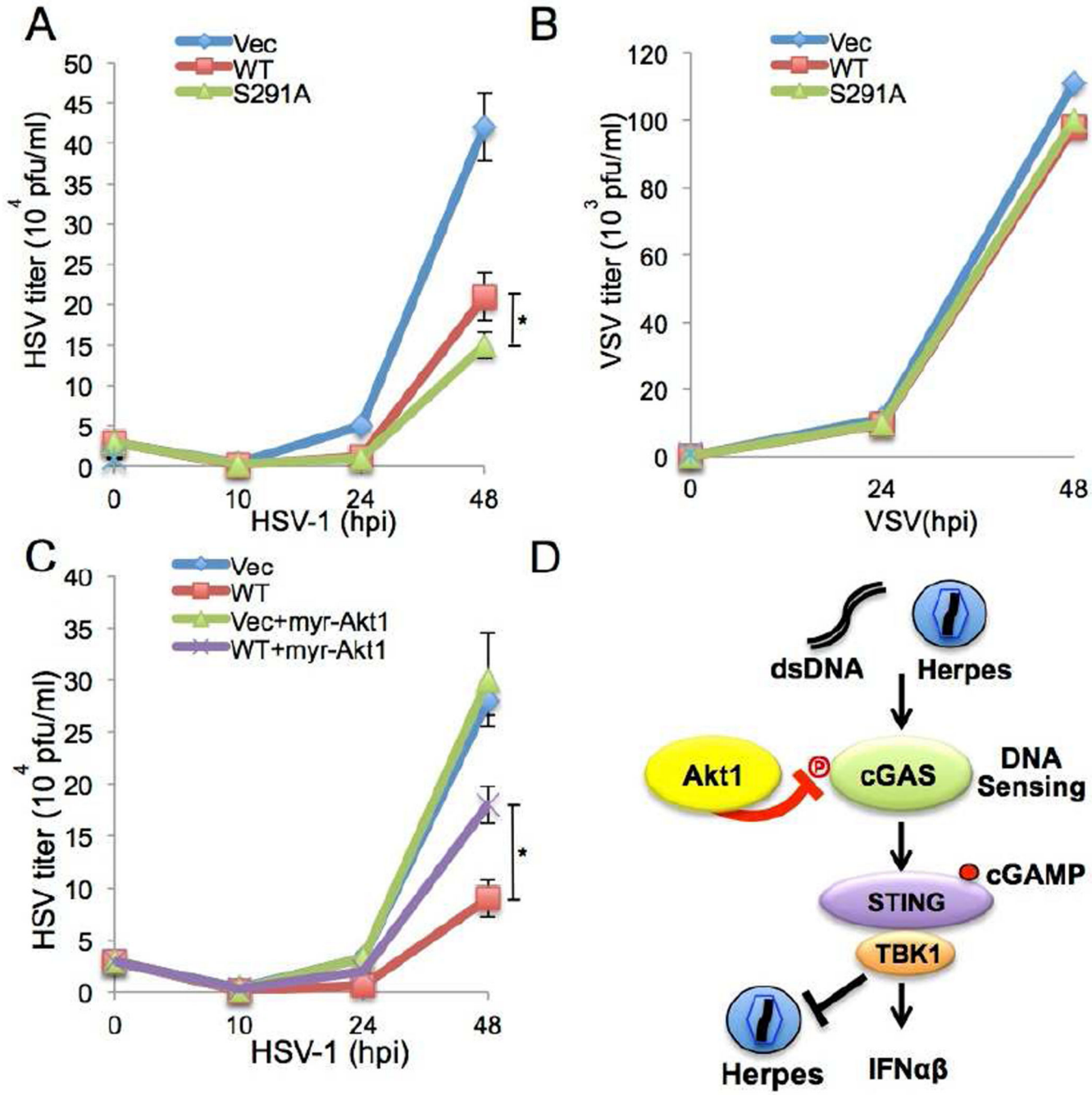

Figure 6. The negative regulation of cGAS antiviral activity by Akt upon virus infection

(A–B) The S291A mutation enhances cGAS-mediated antiviral activity toward HSV-1 infection. L929 cGAS−/− cells stably complemented with empty vector, mouse cGAS WT (mWT) or S291A were infected with HSV-1 (moi = 0.1, A) or VSV (moi = 0.1, B). Viral supernatants were collected at indicated times and titered using plaque assays on Vero cells. (C) Stable myr-Akt1 expression inhibits cGAS activity, leading to high viral replication. L929 cGAS−/− cells stably complemented with empty vector or mouse cGAS WT (mWT)

were infected with HSV-1 (moi = 0.1). Viral supernatants were collected at indicated times and titered using plaque assays on Vero cells. * $p<0.05$.
(D) Proposed model for the functional role of Akt in cGAS-mediated cytokine production and antiviral activity.